〈報文〉 HWAHAK KONGHAK Vol. 17, No. 3, June 1979, pp. 167—178
(Journal of the Korean Institute of Chemical Engineers)

# 수평식 역삼투관에서의 자연대류 현상

임 선 기
한국과학원 화학공학과
(접수 1979. 1. 30)

# Free Convection Dominant Asymptotic Region in a Horizontal Tubular Reverse Osmosis

**Son-Ki Ihm**

*Department of Chemical Engineering*
*Korea Advanced Institute of Science, Seoul 131, Korea*
(Received January 30, 1979)

## 요 약

수평식 관형 Reverse Osmosis에서 격막을 통한 물의 생산량은 축방향에 따라 감소한다는 종래의 해석과는 달리, 입구에서 조금 지나면 일정해진다는 것이 여러 실험결과로 부터 알려지고 있는데, 이것은 농도차이로 인한 자연 대류 현상때문이라고 믿어진다. Prandtl 수가 큰 경우의 열전달 문제에 이미 적용되었던 것과 마찬가지 방법의 무차원 해석으로 부터 간략화되어 얻어진 이차 운동에 관한 편미분 방정식을 적분방법으로 풀었다. 농도 Polarization과 물의 투과속도를 Reverse Osmosis의 성능으로 볼 때, 관의 맨윗쪽이 관벽 주위의 다른 위치에서 보다 더 좋은 것으로 나타났다. 얻어진 결과로 부터, 사입유체의 농도, 운전압력, 관의 직경이 성능에 미치는 영향을 예측할 수 있다.

## Abstract

Axial invariance of production performance encountered in a horizontal tubular reverse osmosis has been analyzed by assuming that the free convection is the dominant transport mechanism. The governing equations, which had been deduced from dimensional analyses used in heat transfer problem with a large Prandtl number, have been solved approximately by the integral method. The numerical computations show that the system performance in terms of concentration polarization and wall permeation velocity, even if axially constant, is better at the top of the tube than at any other circumferential positions. The effects of system parameters such as

feed concentration level, operating pressure and tube radius can also be explained from the results obtained.

## Introduction

The importance of free convection effect in a reverse osmosis system has been cited by some investigator[1)~3)], since the experimental performance is much better than that predicted by the forced convection only models[4)~6)].

Derzansky and Gill[7)] showed, from their experiments for a horizontal tubular reverse osmosis unit, that the system behavior is almost constant over the down-stream region of laminar flow and dictated by combined free and forced convection mechanisms.

Some theoretical analyses on the free convection effect in reverse osmosis have been made. Notably Ramanadhan and Gill[8)] solved the combined free and forced convection problem in a vertical semipermeable parallel plate ducts by a perturbation method. Johnson and Acrivos[9)] obtained the concentration polarization at the wall on a vertical flat membrane by using a series expansion including the similarity variable. Srinivasan and Tien[10)] applied the integral method to solve the reverse osmosis problem consisting of a vertical membrane with a liquid stream flowing upward.

Recently Chang and Guin[11)] examined the influence of combined forced and free convection on the performance of a reverse osmosis system in a horizontal pipe. They used the axial velocity profile proposed by Berman[12)] which introduces three dimensional character into the secondary motion. Perturbation equations were solved numerically by stream function-vorticity scheme, while nonperturbation equations are explained by approximate solutions obtained from the literature[4)~6),13),14)].

In the present analysis, however, the integral method is applied over the boundary layer near the membrane. Only asymptotic region is considered and, with the axial dependence neglected, the problem can be described by two dimensional equations. Effect of free convection over the downstream region under laminar flow through a horizontal tubular reverse osmosis system is analyzed. The velocity distribution to the mass transfer section is assumed fully-developed and the feed concentration is uniform and very dilute as in a sea water.

## Secondary Flow

It is believed that the free convection due to concentration polarization at the membrane surface causes secondary motion, whose flow pattern seems to be symmetric about a vertical plate passed through the axis of the tube, being superimposed on the primary flow in the direction of tube axis.

The above mentioned assumption is evidenced by the pictures taken by Mori and Futagami[15),16)] from their flow visualization experiments for heat transfer. Hot air flowing inside the horizontal tube was cooled at the tube wall with constant heat flux. The secondary motion is downward within the boundary layer near the wall and upward in the core region of the tube. Although there is a mass permeation through the wall in reverse osmosis, the system behavior seems to be sim-

ilar to that for heat transfer problem with large Prandtl number, because Schmidt number is generally very large for reverse osmosis; for example, it is about 700 for sea water.

In the thin boundary layer, velocity and concentration distributions are affected by viscosity and molecular diffusivity, and boundary layer approximation may be applied in an analysis. On the other hand, in the core region, velocity and concentration fields are affected mainly by the secondary flow and the effects of viscosity and molecular diffusivity may be neglected. Because there is a leakage of solvent through the wall, the axial velocity profile is affected along the axial distance[12]. However, any axial variations of secondary flow fields can be neglected as far as the permeating flux is small.

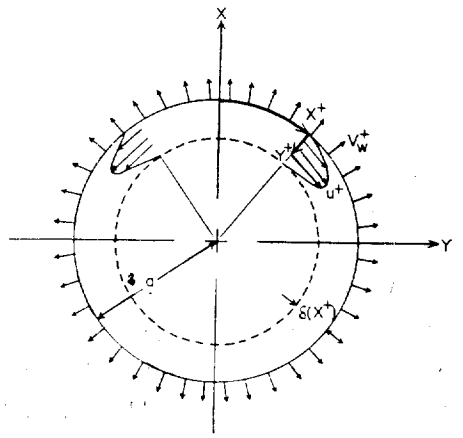


**Fig. 1. Schematic Diagram for the Coordinate** (The boundary layer thickness is a function of $X^+$. The velocity profile is not an exact representation but a symbolic one showing that the velocity field is confined in the boundary layer)

## Formulation of Problem

For the sake of analysis, the coordinates are defined for the core region and for the boundary layer region separately as shown in *Fig.* 1.

For the core region the usual rectangular coordinates are defined. For the boundary layer, which is more important in the following discussions, $X^+$ is the circumferential distance from the top of the tube and $Y^+$ is the normal distance from the membrane surface toward the center of the tube. $U^+$ and $V^+$ are the velocity components in the direction of $X^+$ and $Y^+$ respectively.

The tube radius is $a$ and the thickness of the boundary layer is $\delta$ which is a function of $X^+$. The feed concentration is $C_0$ and the wall permeation velocity is $V_W{}^+$, being a negative quantity.

If natural convection is assumed to be the dominant transport mechanism, and if the core concentration to be uniform and not much different from the feed concentration, the limiting equations in the concentration boundary layer become

$$\frac{\partial U^+}{\partial X^+}+\frac{\partial V^+}{\partial Y^+}=0 \tag{1}$$

$$0=\beta g(C-C_0)\sin\frac{X^+}{a}+\frac{\mu}{\rho_0}\frac{\partial^2 U^+}{\partial Y^{+2}} \tag{2}$$

$$U^+\frac{\partial C}{\partial X^+}+V^+\frac{\partial C}{\partial Y^+}=D\frac{\partial^2 C}{\partial Y^{+2}} \tag{3}$$

with the associated boundary condition being given by

$$U^+=0;\ V^+=V_W{}^+;\ C=C_W \text{ at } Y^+=0$$

$$\frac{\partial U^+}{\partial Y^+}=\frac{\partial C}{\partial Y^+}=0;\ C=C_0 \text{ at } Y^+=\delta$$

$$\frac{d\delta}{dX^+}=0 \text{ at } X^+=0$$

Equations (1) to (3) are obtained through dimensional analysis similar to that applied to heat transfer problem for a large Prandtl number[17]. The process for dimensional analysis is too complicated to be introduced in the present paper but it is only mentioned

here that one of the criteria for the simplification is a large value of $Sc/Pe$, which is valid for the reverse osmosis as will be shown in the next section.

The wall permeation velocity can be given by Merten's phenomenological expression[15]

$$V_W^+ = -K[\Delta P - (\pi_w - \pi_p)] \quad (4)$$

where $\Delta P$ is the difference in static pressure across the membrane, and $\pi_w$ and $\pi_p$ are the osmotic pressures corresponding to the solute concentrations at the membrane surface and at the product side respectively, and $K$ is the water permeability constant. Additionally, the general boundary condition at the high pressure side of the solution/membrane interface is given by

$$N_W = -\rho C_p V_W^+ = \rho D \frac{\partial C}{\partial Y^+}\Big|_{Y^+=0} - \rho C_W V_W^+ \quad (5)$$

Eq. (5) implies that the salt flux to the membrane on the solution side is equal to the salt flux on the product side.

## Dimensional Analysis

Dimensionless variables and groups are defined as follows:

$$x^+ = \frac{X^+}{a},\ y^+ = \frac{Y^+}{\delta_c},\ \Delta^+ = \frac{\delta}{\delta_c},$$

$$u^+ = \frac{U^+}{u^+},\ v^+ = \frac{V^+}{v^+},\ \phi = \frac{C - C_0}{C_0},$$

$$Gr = \frac{\beta a^3 g C_0}{\nu_0^2},\ Sc = \frac{\nu_0}{D},\ Pe = \frac{ua}{D}$$

where $u$ is the characteristic core velocity, and $u^+$ and $v^+$ are the characteristic boundary layer velocities in the $X^+$ and $Y^+$ directions respectively, and $\delta_c$ is the characteristic boundary layer thickness.

The characteristic quantities can be obtained by assuming that the viscous and buoyancy terms in the $X^+$-momentum equation and convection and diffusion terms in the mass balance equation are of the same magnitude.[17),19)] The results obtained together with the continuity equation become

$$\delta_c = \frac{a}{(Gr \cdot Sc)^{\frac{1}{4}}}$$

$$u^+ = \frac{\nu_0}{a}\left(\frac{Gr}{Sc}\right)^{\frac{1}{2}}$$

$$v^+ = \frac{\nu_0}{a}\left(\frac{Gr}{Sc^3}\right)^{\frac{1}{4}}$$

The characteristic core velocity $u$ can be evaluated by assuming that the secondary motion is confined in the boundary layer (i.e., $u^a = u^+\delta_c$), and given by

$$u = \frac{\nu_0}{a}\left(\frac{Gr}{Sc^3}\right)^{\frac{1}{4}} [\equiv v^+]$$

$Sc/Pe$ becomes $(Sc^3/Gr)^{\frac{1}{4}}$ whose typical value is around $\theta(10)$. Therefore the criterion mentioned in the previous section is satisfied.

The governing equations are written in dimensionless form as follows

$$\frac{\partial u^+}{\partial x^+} + \frac{\partial v^+}{\partial y^+} = 0 \quad (6)$$

$$0 = \phi \sin x^+ + \frac{\partial^2 u^+}{\partial y^{+2}} \quad (7)$$

$$u^+ \frac{\partial \phi}{\partial x^+} + v^+ \frac{\partial \phi}{\partial y^+} = \frac{\partial^2 \phi}{\partial y^{+2}} \quad (8)$$

with the boundary conditions being given by

$$u^+ = 0;\ v^+ = v_w^+;\ \phi = \phi_w \text{ at } y^+ = 0$$

$$\frac{\partial u^+}{\partial y^+} = \frac{\partial \phi}{\partial y^+} = \phi = 0 \text{ at } y^+ = \Delta^+$$

$$\frac{d\Delta^+}{dx^+} = 0 \text{ at } x^+ = 0$$

The dimensionless permeation velocity is written as

$$v_w^+ = -\frac{1}{B_2 \chi}[1 - RB_2(1 + \phi_w)] \quad (9)$$

where $B_2 = \frac{\pi_0}{\Delta P}$

$$\chi = \frac{\nu_0}{a}\left(\frac{Gr}{Sc^3}\right)^{\frac{1}{4}} / K\pi_0$$

and $R = 1 - \frac{C_p}{C_w}$

$B_2$ is the ratio of osmotic pressure corresponding to the feed concentration $C_0$ and the static pressure difference, and $\chi$ is dimensionless velocity. $R$ is called rejection parameter

and assumed to be constant in this study. The system can be characterized by these three parameters.

On the other hand, the wall boundary condition is given by

$$\left.\frac{\partial\phi}{\partial y^+}\right|_{y^+=0}=R(1+\phi_w)v_w^+ \tag{10}$$

Exact solutions for the set of differential equations (Eqs. (6) through (10)) can not be obtained. The following section is concerned with an approximate analyses using integral method.

## Solution by Integral Method

The convective diffusion equation (Eq. (8)) is integrated over the boundary layer thickness in conjunction with Eq. (6) to give

$$\frac{d}{dx^+}\int_0^{\Delta^+}u^+\phi dy^+-\phi_w^+v_w^+=-\left.\frac{\partial\phi}{\partial y^+}\right|_{y^+=0} \tag{11}$$

Let the dimensionless concentration profile have the following form:

$$\phi=\phi_w\cdot Y(\eta) \tag{12}$$

where $\eta=\frac{y^+}{\Delta^+}\left(=\frac{Y^+}{\delta}\right)$ (13)

and $Y(\eta)$ can be chosen as

$$Y(\eta)=(1-\eta)^2 \tag{14}$$

satisfying the boundary conditions ($Y(0)=1$, $Y(1)=Y'(1)=0$).

The circumferential velocity profile can be obtained by integrating the momentum equation (Eq. (7))

$$u^+=-\phi_w\cdot\sin x^+\cdot\Delta^{+2}\cdot K(\eta) \tag{15}$$

where

$$K(\eta)=\int_0^\eta\int_1^\eta Y(\eta')d\eta'd\eta \tag{16}$$

$$\left(=-\frac{1}{3}\eta+\frac{1}{2}\eta^2-\frac{1}{3}\eta^3+\frac{1}{12}\eta^4\right)$$

satisfying the boundary condition ($K(0)=K'(1)=0$).

At this point, a comment may be appropriate regarding the aforementhioned profile for $u^+$. At the edge of the boundary layer ($y^+=\Delta^+$ and $\phi=0$), Eq. (7) results in

$$\frac{\partial^2u^+}{\partial y^{+2}}=0 \qquad \text{at } y^+=\Delta^+$$

This implies that, at the matching region of the core and boundary layer, the velocity profile has both inflection $\left(\left.\frac{\partial^2u^+}{\partial y^{+2}}\right|_{y^+=\Delta^+}=0\right)$ and maximum or minimum $\left(\left.\frac{\partial u^+}{\partial y^+}\right|_{y^+=\Delta^+}=0\right)$. Siegwarth *et al*[17] suggested that the inflection point approach the max. or min. point. Two cases[17] may be considered as shown in *Fig.*2.

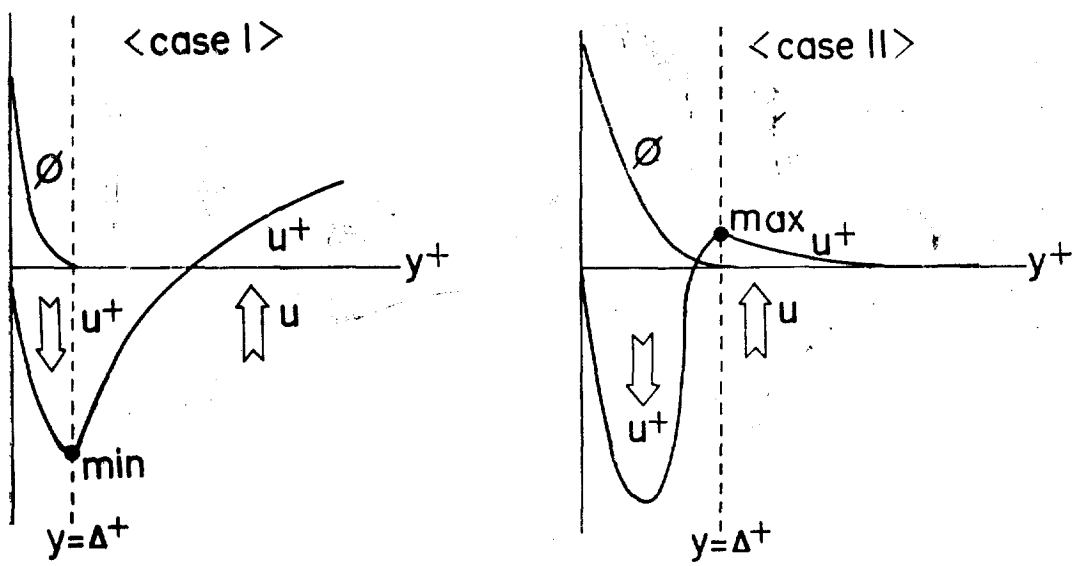


**Fig. 2. Schematic Diagram of Dimensionless Velocity Profile near the Membrane.**

In case I, the downstream velocity is of the same order of magnitude as the upstream one (i.e., $u^+=u$), while in case II the downstream velocity is confined in the boundary layer (i.e., $u^+\delta=ua$). Case II is more reasonable in view of the criterion of $Sc/Pe\to\infty$ because $Pe=(Gr\cdot Sc)^{\frac{1}{2}}$ for case I and $Pe=(Gr\cdot Sc)^{\frac{1}{4}}$ for case II, and another forms of $Y(\eta)$ can be chosen by assuming $u^+(\Delta^+)=0$ (i.e., $K(1)=0$) and from Eq. (8) $\frac{\partial^2\phi}{\partial y^{+2}}\Big|_{y^+=\Delta^+}=0$ (i.e., $Y''(1)=0$). However it should be stressed that integral method for the boundary layer is an approximate approach and the more complicated profile does not necessarily improve the estimation.

The substitution of Eqs. (10), (12) and (15) into Eq. (11) leads to the following differential equation

$$\sin x^+\cdot\Delta^{+2}(2\phi_w'\Delta^+ +3\phi_w)\frac{d\Delta^+}{dx^+}$$

$$=-\cos x^+\cdot\Delta^{+3}\cdot\phi_w-43\left(\frac{R}{\phi_w}-1+R\right)v_w^+ \quad (17)$$

where $\phi_w'=\frac{d\phi_w}{d\Delta^+}$

Initial condition to Eq. (17) is given by

$$\frac{d\Delta^+}{dx^+}\Big|_{x^+=0}=0,$$

which implies that the boundary layer thickness is symmetric at the top of the tube. From Eq. (17), we obtain

$$\Delta^{+3}=-43\left(\frac{R}{\phi_w}-1+R\right)\cdot\frac{v_w^+}{\phi_w}$$

at $x^+=0$ (18)

In addition, the wall boundary condition (Eq. (10)) becomes

$$\phi_w\frac{Y'(0)}{\Delta^+}=R(1+\phi_w)v_w^+, \quad (19)$$

and the dimensionless wall velocity is related to the dimensionless wall concentration through Eq. (9).

Now it is possible to solve Eq. (17) together with Eqs. (9), (18) and (19). Runge-Kutta method[20] was used for the numerical computations. The boundary layer thickness becomes infinity at the bottom of tube ($x^+=\pi$) which is the singular point of Eq. (17).

Once the circumferential variation of $\Delta^+$ is known, $\phi_w(x^+)$ and $v_w^+(x^+)$ are obtained directly from Eqs. (9) and (19). The circumferential averages are defined by

$$\bar{\phi}_w=\frac{1}{\pi}\int_0^\pi\phi_w(x^+)dx^+ \quad (20)$$

and $$\bar{v}_w^+=\frac{1}{\pi}\int_0^\pi v_w^+(x^+)dx^+ \quad (21)$$

*Fig.* 3 shows how the ratio of the wall concentration and the permeation velocity to the circumferential averages change along the wall position from the top to the bottom of the tube. The concentration polarization increases and the permeation velocity decreases as the circumferential position moves from the top to the bottom of tube. The performance in terms of solvent production can be said to be better at the top of the tube than at any other circumferential positions.

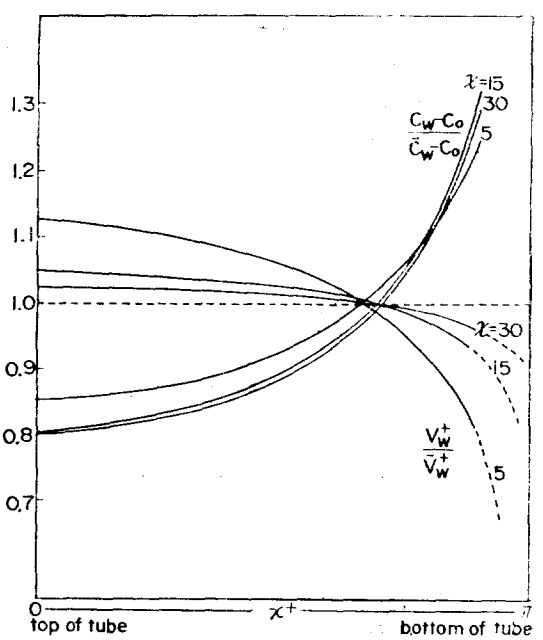


**Fig. 3. Circumferential Variation of Dimensionless Wall Concentration, $(\bar{C}_W-\bar{C}_0)/(C_W-C_0)$, and Dimensionless Wall Permeation Velocity, $V_W^+/\bar{V}_W^+$ for $R=1.0$ and $B_2=0.2$**

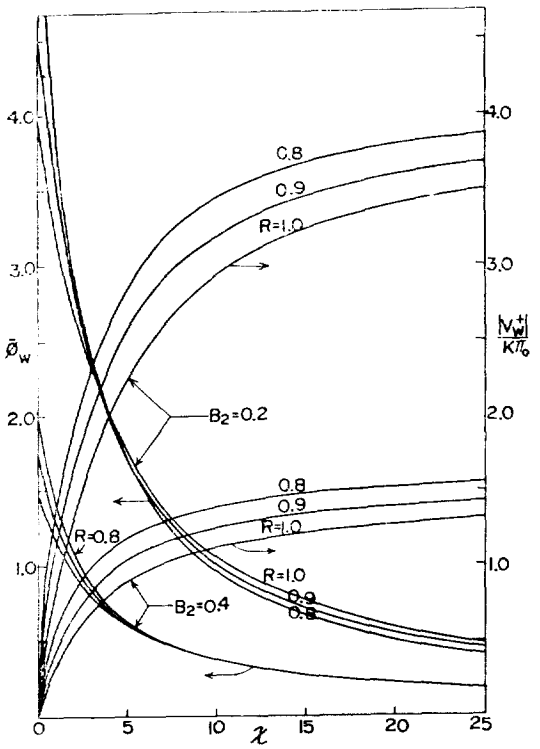


**Fig. 4. Concentration Polarization $\phi_w$ and Dimensionless Wall Permeation Velocity $|V_W^+|/K\pi_0$ for Varying System Parameters**

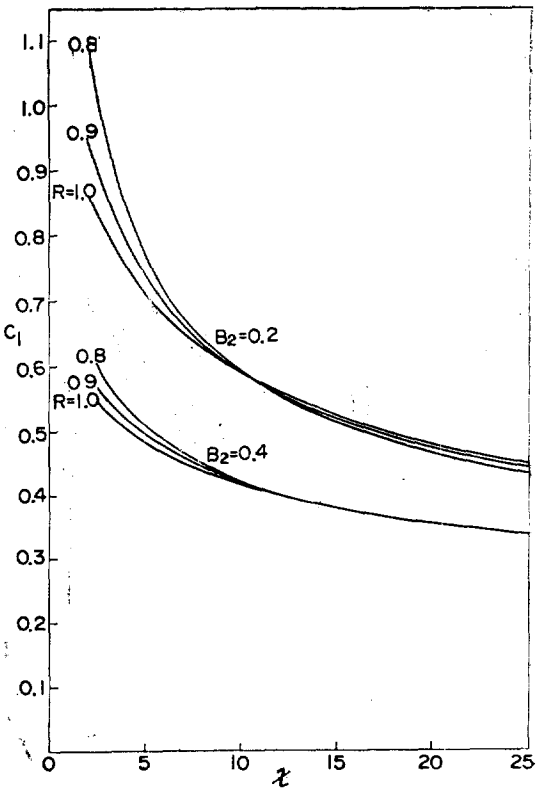


**Fig. 5. $C_1$ for Varying System Parameters**

*Fig.* 4 shows how $\bar{\phi}_w$ and $\frac{|\bar{V}_w^+|}{K\pi_0}$ (being equal to $|\bar{v}_w^+|\chi$) change with the system parameters, whose effects are discussed in the later section.

## Sherwood Number Correlation

If the local mass transfer coefficient[21] is defined by

$$k_l=\frac{-D\left.\frac{\partial C}{\partial Y^+}\right|_{Y^+=0}}{C_w-C_0}, \tag{22}$$

Sherwood number ($Sh$) becomes

$$Sh_l\left(\equiv\frac{k_l a}{D}\right)=\left(-\frac{1}{\phi_w}\cdot\left.\frac{\partial\phi}{\partial y^+}\right|_{y^+=0}\right)\cdot(Gr\cdot Sc)^{\frac{1}{4}} \tag{23}$$

The average Sherwood number is given by

$$Sh\left(\equiv\frac{1}{\pi}\int_0^\pi Sh_l dx^+=C_1\cdot(Gr\cdot Sc)^{\frac{1}{4}}\right) \tag{24}$$

where

$$C_1=\frac{1}{\pi}\int_0^\pi\frac{Y'(0)}{\Delta^+}dx^+ \tag{25}$$

*Fig.* 5 shows that $C_1$ decreases as $B_2$ increases, and that for small values of $\chi$, $C_1$ is very sensistive to rejection parameter and that for large values of $\chi$, insensitive to $R$.

## Effect of System Parameters

The system performance in terms of $C_1$ increases as $R$ decreases (except for small $B_2$ with large $\chi$) and as $B_2$ and $\chi$ decrease as shown in *Fig.* 5. The effect of rejection for small $B_2$ with large $\chi$ is reversed; as $R$ decreases, the performance becomes worse, which is consistent with the results for the asymptotic case of $B_2=0$ discussed in next section. However, $C_1$ is independent of $R$ for the values of $\chi$ larger than 15 for $B_2=0.4$.

As $C_0$ and $\Delta P$ increase at the same time so that $B_2$ remains constant and $\chi$ decreases, the performance is improved even if the concentration polarization becomes larger. This implies that the effect of increase in operating pressure overcomes the increased barrier to solvent transport due to higher concentration polarization.

The geometric effect of tube radius can be analyzed by changing $\chi$ which is proportional to $a^{1/4}$ As $a$ increases (and so $\chi$ decreases), $C_1$ increases. However, the concentration polarization increases and dimensionless wall velocity decreases. The enhancement of free convection due to the large tube radius is canceled out by the rapid increase in the boundary layer thickness.

Among the system parameters, the effect of rejection seems to be less important especially when $B_2$ and $\chi$ are large even if it directly affects the product quality.

## Analysis for the Case of $B_2=0$

$B_2=0$ is an asymptotic case where the feed concentration is very dilute while the operating pressure is high. Because the wall permeation velocity is constant(i.e., $V_w^+=-K$-$\Delta P$), $v_w^+$ is itself a parameter. The system performance is uniform around the tube wall.

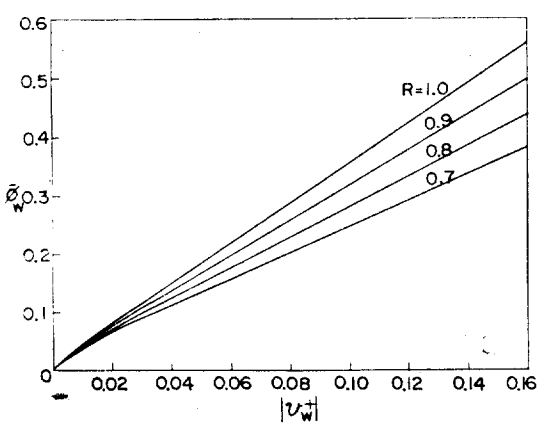


**Fig. 6. Concentration Polarization for $B_2=0$**

The effects of rejection parameter on the concentration polarization and $C_1$ are shown in *Fig.* 6 and *Fig.* 7. As $R$ increases, both concentration polarization and $C_1$ increase. The trend of this result is in agreement with that predicted by the forced convection only model [4~6].

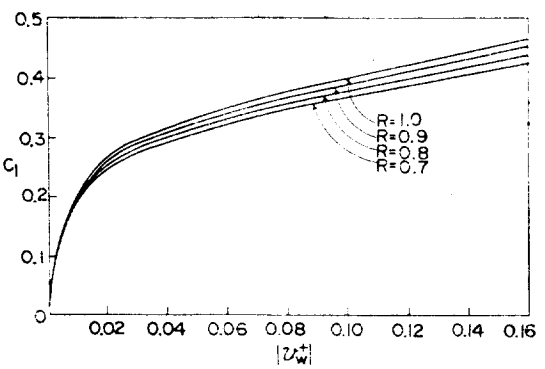


**Fig. 7. $C_1$ for $B_2=0$**

## Discussion

Chang and Guin[11] obtained the Sherwood number correlation for $R=1.0$ and $B_2=0$ by converting their local Sherwood numbers through film theory into asymptotic ones for no wall permeation, being expressed as

$$Sh_{0(C-G)}=0.863[|v_w|\cdot(Gr\cdot Sc)]^{0.166} \quad (26)$$

where $v_w=-\dfrac{K\Delta Pa}{D}$. Note that the Sherwood number here is based on the tube radius instead of the diameter.

Similar correlation can be obtained here from the result by the integral method, since the value of $C_1$ in Eq. (24) (i.e., $Sh=C_1(Gr\cdot Sc)^{\frac{1}{4}}$) is depending upon the system parameters. Especially for $R=1.0$ and $B_2=0$, $C_1$ is a function of only $|v_w^+|$, which is equal to $|v_w|(Gr\cdot Sc)^{-\frac{1}{4}}$. We fit the courve for $R=1.0$ and $B_2=0$ in *Fig.* 7 according to

$$C_1=0.588|v_w^+|^{0.2} \quad (27)$$

which was found to be a good correlation for the values of $|v_w^+|$ less than 0.04. According to the film theory, the asymptotic Sherwood number is related to the local Sherwood number by

$$Sh=\theta_{AB}Sh_0 \tag{28}$$

where correction factor $\theta_{AB}$ is given by Bird *et al*[21] as

$$\theta_{AB}=\phi_{AB}/[\exp\ \phi_{AB}-1] \tag{29}$$

and the rate factor $\phi_{AB}$ is defined by

$$\phi_{AB}=-\frac{|\bar{V}_W|\delta}{D} \tag{30}$$

From $|\bar{V}_W|=K\Delta P$ for $B_2=0$ and $\delta=a/(Gr\cdot Sc)^{\frac{1}{4}}$, we find

$$\phi_{AB}=-|v_w^+| \tag{31}$$

The asymptotic Sherwood number becomes

$$Sh_0=\frac{C_1(Gr\cdot Sc)^{\frac{1}{4}}}{\dfrac{-|v_w^+|}{\exp(-|v_w^+|)-1}} \tag{32}$$

For $|v_w^+|\ll 1$, $\exp(-|v_w^+|)=1-|v_w^+|$, and Eq. (32) together with Eq. (27) can be written as

$$Sh_0\simeq C_1(Gr\cdot Sc)^{\frac{1}{4}}$$

$$\text{or } Sh_0\simeq 0.588[|v_w|\cdot(Gr\cdot Sc)]^{0.2} \tag{33}$$

Once the asymptotic Sherwood number is obtained, the axial onset position of free convection dominant region can be estimated by equating the theoretical Leveque solution for the inlet region where the forced convection is the dominant transport mechanism. The Leveque type solution is given by

$$Sh_{0(\text{Leveque})}=\frac{1.301}{2}z^{-\frac{1}{3}} \tag{34}$$

where $z=\dfrac{DZ}{4\langle \bar{W}_0\rangle a^2}$ is dimensionless axial distance. From Eqs (26) and (34), Chang and Guin[11] give the axial onset position as

$$Z_{tr(C-G)}=0.753[|v_w|(Gr\cdot Sc)]^{-0.166} \tag{35}$$

From the present analysis, $Z_{tr}$ becomes

$$Z_{tr}=1.1\times(|v_w|(Gr\cdot Sc))^{-0.2} \tag{36}$$

## Summary

Free convection in a horizontal tubular reverse osmosis is known as a dominant transport mechanism over the downstream region of laminar flow. Chang and Guin[11] solved the pertubation equations numerically by stream function-vorticity scheme, accounting for the axial dependence of axial velocity profile. In the present paper, however, the integral method is applied to the concentration boundary layer near the membrane and, the secondary motion was described by two dimensional equations according to the experimental findings of axial invariance in the performance of reverse osmosis.

The velocity field at the inlet to mass transfer section was assumed to be fully-developed and the feed concentration to be very dilute and uniform. Numerical solutions show that at the top of the tube the concentration polarization is smaller and the permeation velocity is larger than at any other circumferential positions. Also the effects of system parameters such as feed concentration level, operating pressure and tube radius can be explained from the results obtained.

## Acknowledgement

This work was completed as part of author's M.S. thesis at the State University of New York at Buffalo in U.S.A. It is acknowledged that the author took advantage of critical comments from one of the evaluation committee in the process of revision.

## Nomenclature

$a$ tube radius(cm)

$B_2$ ratio of osmotic pressure of feed solution to the difference of static pressure, i.e., $\pi_0/\Delta P$

$C$ solute concentration in mole fraction

$C_0, C_W, C_p$ solute concentrations in the feed, at the membrane surface and in the product respectively

$C_1$ correlation coefficient for Sherwood number, i.e., $Sh/(Gr\cdot Sc)^{\frac{1}{4}}$

$D$ molecular diffusivity of solute($cm^2/sec$)

$g$ gravitational acceleration

$Gr$ Grashof number defined by $a^3\beta g C_0/\nu_0^2$

$K$ water permeability constant of membrane (cm/sec/psi)

$k_l$ local mass transfer coefficient(cm/sec)

$N_w$ local salt flux on the product side

$Pe$ Peclet number defined by $au/D$

$\Delta P$ difference in static pressure across the membrane(psi)

$R$ rejection parameter defined by $1-C_p/C_w$

$Sc$ Schimidt number defined by $\nu_0/D$

$Sh_l$ local Sherwood number defined by $k_l a/D$

$Sh$ circumferentially averaged Sherwood number

$Sh_0$ asymptotic Sherwood number for no wall permeation

$Sh_{0(Leveque)}$ Sherwood number obtained for inlet region from Leveque solution

$u$ characteristic core velocity for the secondary flow defined by

$$\frac{\nu_0}{a}\left(\frac{Gr}{Sc^3}\right)^{\frac{1}{4}}\left[\equiv\frac{D}{a}(Gr\cdot Sc)^{\frac{1}{4}}\right]$$

$u^+$ characieristic circumferential velocity in the $X^+$ direction for the bounday layer defined by

$$\frac{\nu_0}{a}\left(\frac{Gr}{Sc}\right)^{\frac{1}{2}}\left[\equiv\frac{D}{a}(Gr\cdot Sc)^{\frac{1}{2}}\right]$$

$U^+$ circumferential velocity in the $X^+$ direction

$u^+$ dimensionless circumferential velocity defined by $U^+/u^+$

$v^+$ characteristic velocity in the $Y^+$ direction for the boundary layer defined by

$$\frac{\nu_0}{a}\left(\frac{Gr}{Sc^3}\right)^{\frac{1}{4}}[\equiv u]$$

$V^+$ velocity in the $Y^+$ direction

$V_W^+$ water permeation velocity through the membrane

$v^+$ dimensionless velocity defined by $V^+/v^+$

$v_w$ dimensionless permeation velocity for $B_2=0$ defined by $-\dfrac{K\Delta Pa}{D}$

$v_w^+$ dimensionless permeation velocity defined by $V_W^+/v^+$

$\langle W_0\rangle$ bulk averaged axial velocity

$X^+$ boundary layer coordinate in the circumferential distance from the top of the tube

$x^+$ dimensionless boundary layer coordinate defined by $X^+/a$

$Y^+$ boundary layer coordinate perpendicular to the wall inwards

$y^+$ dimensionless boundary layer coordinate defined by $Y^+/\delta_c$

$Z$ axial distance

$z$ dimensinless axial position defined by $\dfrac{DZ}{4a^2\langle W_0\rangle}$

$z_{tr}$ dimensionless transition length for the onset of asymptotic region

**Greek letters**

$\beta$ volumetric expansion coefficient due to concentration difference

$\delta$ concentration boundary layer thickness

$\delta_c$ characteristic boundary layer thickness defined by $\dfrac{a}{(Gr\cdot Sc)^{\frac{1}{4}}}$

$\Delta^+$ dimensionless boundary layer thickness defined by $\delta/\delta_c$

$\eta$ similarity variable defined by $y^+/\Delta^+(=Y^+/\delta)$

$\theta_{AB}$ correction factor for the film theory

$\mu$ viscosity

$\nu_0$ kinematic viscosity defined by $\mu/\rho_0$

$\pi_0, \pi_w, \pi_p$ osmotic pressures of solution with corresponding concentration $C_0, C_w$ and $C_p$ respectively

$\rho$ solution density (g/cm³)

$\phi$ dimensionless concentration defined by $\frac{C-C_0}{C_0}$

$\phi_w$ dimensionless wall concentration defined by $\frac{C_w-C_0}{C_0}$

$\bar{\phi}_w$ concentration polarization defined by $\frac{\bar{C}_w-C_0}{C_0}$ or the circumferential average of $\phi_w$

$\phi_{AB}$ rate constant for $\theta_{AB}$

$\chi$ dimensionless velocity defined by $v^+/K\pi_0$

## References


1. T.J. Hendricks, J.F. Macquin and F.A. Williams, *I & EC Fund.*, **11**(1972) 276.
2. L.E. Monge, M.S. Thesis, Univ. of California (Davis), 1972.
3. J.L. Richardson, G. Segovia, W.Baerg and M. Anderson, "Reverse Osmosis Tubular Module Optimization", Office of Saline Water, U.S. Department of the Interior, Res. Develop. Rept. No. 455, 1969.
4. W.N. Gill, C. Tien and D.W. Zeh, *Int. J. Heat Mass Transfer*, **9**(1966) 907.
5. R.A. Shaw, R. Deluca and W.N. Gill, *Desalination*, **11**(1972) 189.
6. P.L.T. Brian, *I & EC Fund.*, **4**(1965) 439.
7. L.J. Derzansky and W.N. Gill, *AIChE J.*, **20**(1974) 751.
8. K. Ramanadhan and W.N. Gill, *AIChE J.*, **15**(1969) 872.
9. A.R. Johnson and A. Acrivos, *I & EC Fund.*, **8**(1969) 359.
10. S. Srinivasan and C. Tien, *Desalination*, **10**(1972) 273
11. C.Y. Chang and J.A. Guin, *AIChE J.*, **24** (1978) 1046.
12. A.S. Berman, *J. Appl. Physics*, **24**(1953) 1232.
13. L. Dresner, "Boundary Layer Build-up in the Demineralization of Salt Water by Reverse Osmosis", Oak Ridge National Lab, Rept. 3621, May, 1964.
14. W.N. Gill L.T. Derzansky and M.R. Doshi, "Mass Transfer in Laminar and Turbulent Flow Hyperfiltration Systems", Office of Saline Water, U.S. Dept. of Interior, Res. Develop. Rept. No. 403, 1969.
15. Y. Mori and K. Futagami, *Int. J. Heat Mass Transfer*, **10**(1967) 1801.
16. Y. Mori, K. Futagami, S. Tokuda and M. Nakamura, *Int. J. Heat Mass Transfer*, **9**(1966) 453
17. D.P. Siegwarth, R.D. Mikesell, T.C. Readal and T.J. Hanratty, *Int. J. Heat Mass Transfer*, **12**(1969) 1535.
18. U. Merten, *I & EC Fund.*, **2**(1963) 229.
19. S. Ostrach, NACA Report 1111, 1953.
20. R.L. Ketter and S.P. Prawel, Jr., "Modern Methods of Engineering Computation," McGraw-Hill, 1969, pp. 268.
21. R.B. Bird, W.E. Stewart and E.N. Lightfoot, "Transport Phenemena," Wiley, 1960, Chapter 21.